Published in final edited form as:
*J Immunol*. 2009 May 1; 182(9): 5461–5468. doi:10.4049/jimmunol.0802327.

# Conditional Gene Targeting in Mouse High Endothelial Venules

**Hiroto Kawashima**[2,*,†], **Jotaro Hirakawa**[*], **Yuki Tobisawa**[*], **Minoru Fukuda**[‡], and **Yumiko Saga**[§]

[*]Laboratory of Microbiology and Immunology, School of Pharmaceutical Sciences, University of Shizuoka, Shizuoka, Japan

[†]PRESTO, Japan Science and Technology Agency, Kawaguchi, Japan

[‡]Tumor Microenvironment Program, Cancer Research Center, Burnham Institute for Medical Research, La Jolla, CA

[§]Division of Mammalian Development, National Institute of Genetics, Mishima, Japan

## Abstract

High endothelial venules (HEVs) are specialized blood vessels of secondary lymphoid organs composed of endothelial cells with a characteristic cuboidal morphology. Lymphocytes selectively adhere to and migrate across HEVs to initiate immune responses. In this study, we established a novel transgenic mouse line expressing Cre recombinase under the transcriptional control of the gene encoding HEV-expressed sulfotransferase, *N*-acetylglucosamine-6-*O*-sulfotransferase 2 (GlcNAc6ST-2), using bacterial artificial chromosome recombineering. Crossing these transgenic mice with the ROSA26 reporter strain, which expresses *lacZ* following Cre-mediated recombination, and staining the resulting progeny with 5-bromo-4-chloro-5-indolyl-β-D-galactoside indicated that Cre recombinase was specifically expressed in mAb MECA79-reactive HEVs in secondary lymphoid organs but not in any other blood vessels of the transgenic mice. The expression of Cre recombinase correlated with a developmental switch, from immature, mAb MECA367-reactive HEVs to mature, mAb MECA79-reactive HEVs in neonatal lymph nodes. In addition to the HEVs, Cre recombinase was also strongly expressed in the colonic villi, which recapitulated the intrinsic expression of GlcNAc6ST-2 as confirmed in GlcNAc6ST-2$^{GFP/GFP}$ knock-in mice and by RT-PCR. Furthermore, treatment with an antimicrobial agent revealed that the colonic expression of Cre recombinase in the transgenic mice was regulated by commensal bacteria in the colon. In addition, Cre recombinase was expressed in a small subset of cells in the brain, testis, stomach, small intestine, and lung. In view of the restricted expression of Cre recombinase, this transgenic mouse line should be useful for elucidating tissue-specific gene functions using the Cre/*loxP* system.

Lymphocytes continuously migrate from the bloodstream to secondary lymphoid organs in search of their cognate Ags (1,2). Lymphocytes that emigrate through the lymph return to the bloodstream and migrate again into the secondary lymphoid organs. This circulatory process is called lymphocyte recirculation or lymphocyte homing and is essential for immune surveillance. The lymphocyte migratory process is mediated by sequential adhesive interactions between lymphocytes and specialized postcapillary venules, called high endothelial venules (HEVs),[3] in the secondary lymphoid organs (3).



2Address correspondence and reprint requests to Dr. Hiroto Kawashima, Laboratory of Microbiology and Immunology, School of Pharmaceutical Sciences, University of Shizuoka, 52-1 Yada, Shizuoka 422-8526, Japan. kawashih@ushizuoka-ken.ac.jp.

**Disclosures** The authors have no financial conflict of interest.

Endothelial cells of HEVs have a characteristic cuboidal morphology and a prominent Golgi complex, where unique sulfated glycans are synthesized (4). In contrast to other blood vessels, HEVs specifically express adhesion molecules called vascular addressins, which mediate selective lymphocyte attachment to the HEVs. Two distinct vascular addressins have been described. Peripheral node addressin (PNAd), bearing a sulfated carbohydrate epitope recognized by the mAb MECA-79 (5), mediates lymphocyte attachment to HEVs in peripheral lymph nodes (PLNs) and mesenteric lymph nodes (MLNs), whereas mucosal addressin cell adhesion molecule 1 (MAdCAM-1), recognized by the mAb MECA-367 (6), mediates the lymphocyte attachment to HEVs in Peyer's patches (PP) and MLNs. PNAd and MAd-CAM-1 serve as ligands for the lymphocyte homing receptors L-selectin and $\alpha_4\beta_7$ integrin, respectively (1-3). In early neonates, the phenotype of HEVs in the PLNs switches from a MECA-367-reactive immature type to the MECA-79-reactive mature type (7). The mature HEV phenotype can revert to the immature phenotype during immune reactions in the PLNs, followed by recovery to the mature phenotype (8). In addition, ectopic MECA-79-reactive HEV-like vessels are observed in chronically inflamed nonlymphoid tissues (9,10).

Studies of carbohydrate-based ligands for the lymphocyte homing receptor L-selectin have identified various HEV glycoproteins that are modified with a specific carbohydrate structure called 6-sulfo sialyl Lewis X (sialic acidα2-3Galβ1- 4[Fucα1-3(sulfo-6)]GlcNAcβ1-R) (9). The 6-sulfo sialyl Lewis X structure is present in both *O*- and *N*-glycans (11), both of which function as L-selectin binding sites. The MECA-79 Ab that inhibits L-selectin-mediated lymphocyte binding to HEVs recognizes the extended core 1 *O*-glycans containing 6-sulfo-*N*-acetylglucosamine that are selectively attached to PNAd (12).

To examine the role of carbohydrate sulfation in lymphocyte homing, our group (13) and others (14) have generated gene-targeted mice deficient in both *N*-acetylglucosamine-6-*O*-sulfotransferase 1 (GlcNAc6ST-1) and GlcNAc6ST-2. HEV staining with the MECA-79 Ab is completely eliminated in the double-deficient mice. In addition, an oligosaccharide analysis of HEV-expressed glycoproteins indicated that 6-sulfo sialyl Lewis X is almost completely absent in the double-deficient mice. Consistent with these results, lymphocyte homing to PLNs and contact hypersensitivity responses are significantly lower than normal in these mutant mice, indicating that the sulfation of L-selectin ligands is essential for lymphocyte homing.

The expression of GlcNAc6ST-2 (also called high endothelial cell *N*-acetylglucosamine-6-*O*-sulfotransferase (HEC-GlcNAc6ST) or L-selectin ligand sulfotransferase (LSST)) is restricted to HEVs expressing PNAd (i.e., MECA-79-reactive) (15,16). Liao et al. (17) recently reported that the GlcNAc6ST-2 regulatory sequences drive *lacZ* expression in HEVs in transgenic mice. In this study, to establish an animal model for assessing gene functions in MECA-79-reactive HEVs, we created a transgenic mouse line expressing Cre recombinase under the transcriptional control of the regulatory elements of the gene for GlcNAc6ST-2 using bacterial artificial chromosome (BAC) recombineering (18,19). To evaluate the expression pattern of the Cre recombinase, we crossed the transgenic mice with ROSA26 reporter (R26R) mice (20), in which the *lacZ* gene is transcribed following Cre-mediated recombination. 5-Bromo-4-chloro-3-indolyl-β-D-galactoside (X-gal) staining of the progeny revealed that Cre recombinase was specifically expressed in the MECA-79-reactive HEVs and not in other blood vessels. Cre recombinase was also expressed in the colonic villi of the transgenic mice, which recapitulates the intrinsic expression of GlcNAc6ST-2. We confirmed this expression pattern in knock-in mice that express enhanced GFP (EGFP) under control of the GlcNAc6ST-2 promoter (13,

[3]Abbreviations used in this paper: HEV, high endothelial venule; PNAd, peripheral node addressin; PLN, peripheral lymph node; MLN, mesenteric lymph node; GlcNAc6ST, *N*-acetylglucosamine-6-*O*-sulfotransferase; MAdCAM-1, mucosal addressin cell adhesion molecule 1; PP, Peyer's patch; BAC, bacterial artificial chromosome; X-gal, 5-bromo-4-chloro-3-indolyl-β-D-galactoside; EGFP, enhanced GFP; LB, Luria-Bertani; pAb, polyclonal Ab; Plzf, promyelocytic leukemia zinc finger protein; DDX4, DEAD-box protein 4; Muc2, mucin 2; Sox9, SRY box containing gene 9; AMPC, amoxicillin; NALT, nasal-associated lymphoid tissue.

21) and by RT-PCR. In addition, a modest or lower expression of Cre recombinase was observed in some other tissues. The GlcNAc6ST-2-Cre-transgenic mouse line will be an invaluable tool for studies of tissue-specific gene functions.

## Materials and Methods

### Generation of transgenic mice

A 219,794-bp BAC (RP23-362O14) clone containing the entire gene for mouse GlcNAc6ST-2, purchased from Advanced Geno Techs, was transformed, first with pKD46 (provided by Dr. B. L. Wanner, Purdue University, West Lafayette, IN) encoding the phage λ red recombinase (18), and then with a fragment containing the Cre recombinase and frt-flanked kanamycin-resistance genes flanked by 50-bp homologous sequences of the gene encoding mouse GlcNAc6ST-2. This fragment had been amplified by PCR using the primer pair, 5′-GCCCCATCCCCTCTGCTTGCTCTTTCAAGGTCTTCTCCTTCTTCCGCAGGATGGCCAATTTACTGACCGT-3′ and 5′-TGCGTTTAATGGTGACTAAGGCTGGAACCAAGGGGTGCAGACAGACCTCCGTGTAGGCTGGAGCTGCTTC-3′ and pBKS-CRE-FRTX2-Kan-PS (provided by Dr. M. Oginuma, National Institute of Genetics, Mishima, Japan) as the template encoding Cre recombinase in the frt-flanked kanamycin-resistance gene cassette (22). The BAC clone was then cultured in the presence of 1 mM arabinose to induce the expression of λ red recombinase and selected in the presence of 25 μg/ml kanamycin. Homologous recombination was confirmed by PCR using primers 5′-GATCTGGACAAATACTTGCAGG-3′ (LSST-F), 5′-TAGGCTCAGTTGTAGGGTAGAC-3′ (LSST-R), and 5′-ACGGTCAGTAAATTGGCCAT-3′ (Cre-R). The recombinant BAC was linearized by *I-Sce* I (New England Biolabs) and purified by gel excision after pulse-field electrophoresis. The purified construct was microinjected into the pronuclei of (C57BL/6 × C3H/HeN)$F_1$ mouse zygotes, which were implanted into pseudopregnant foster mothers by standard techniques. The transgenic founder mice were identified by PCR using Cre-specific primers (5′-GGACATGTTCAGGGATCGCCAGGCG-3′ and 5′-GCATAACCAGTGAAACAGCATTGCTG-3′). Four independent founder lines were established and, one of them, GlcNAc6ST-2-Cre, was used for subsequent studies. Mice were treated in accordance with the guidelines of the Animal Research Committee of the University of Shizuoka.

### Whole-mount X-gal staining

PLNs were fixed in PBS containing 2% paraformaldehyde for 30 min and permeabilized with PBS containing 1% Triton X-100 for 30 min. After being washed with PBS containing 0.05% Triton X-100, the tissues were incubated overnight in X-gal solution (1 mg/ml X-gal in PBS containing 5 mM $K_3Fe(CN)_6$,5 mM $K_4Fe(CN)_6$, 2 mM $MgCl_2$, and 0.02% Nonidet P-40) at 37°C with gentle shaking. To stop the reaction, the tissues were washed three times with PBS containing 0.05% Triton X-100.

### Histological analysis

Frozen sections (7 μm) were fixed in PBS containing 1.5% glutaraldehyde for 10 min, incubated overnight with the X-gal solution described above, and stained with Nuclear Fast Red solution (Sigma-Aldrich). In some experiments, tissue sections that had been incubated with X-gal solution were blocked with PBS containing 3% BSA for 30 min and then incubated with 5 μg/ml MECA-79 or MECA-367 (BD Biosciences) for 1 h. After being washed with PBS containing 0.1% BSA, the sections were incubated with methanol containing 0.03% $H_2O_2$ for 5 min to inactivate the endogenous peroxidase. They were then blocked with PBS containing 3% BSA for 30 min and incubated with biotinylated secondary Abs (biotinylated mouse anti-rat IgM diluted 1/100; BD Biosciences) for MECA-79 staining and biotinylated

goat anti-rat IgG F(ab′)$_2$ absorbed with mouse IgG (diluted 1/200; Rockland) for MECA-367 staining, respectively) for 1 h, followed by streptavidin-HRP (Vector Laboratories) diluted 1/500 for 1 h. After the sections were washed with PBS containing 0.1% BSA, the colored reaction product was developed using a metal-enhanced 3,3′-diaminobenzidine substrate kit (Pierce Biotechnology), and the sections were counterstained with Nuclear Fast Red solution. In some experiments, sections of various tissues were stained with rabbit anti-glial fibrillary acidic protein (GFAP) polyclonal Ab (pAb) (Thermo Scientific), biotinylated rat anti-mouse CD11b mAb (BioLegend), goat anti-GATA-4 pAb (Santa Cruz Biotechnology), rabbit anti-SRY box-containing gene 9 (Sox9) pAb (Millipore), rabbit anti-promyelocytic leukemia zinc finger protein (Plzf) pAb (Santa Cruz Biotechnology), rabbit anti-DEAD-box protein 4 (DDX4) pAb (Abcam), or rabbit anti-mucin 2 (Muc2) pAb (Santa Cruz Biotechnology) along with HRP-labeled secondary Abs. Species- and class-matched primary Abs were used as controls.

### Lymphocyte-homing assay

Lymphocyte homing was assayed as described previously, with some modifications (21). In brief, lymphocytes isolated from spleen and MLNs were labeled with CFSE (Invitrogen) and injected into the tail veins of GlcNAc6ST-2-Cre-transgenic mice or their Cre-negative siblings ($2.5 \times 10^7$ lymphocytes/head). After 1 h, lymphocyte suspensions were prepared from the PLNs and MLNs of each mouse and were analyzed by flow cytometry (FACS Canto II; BD Biosciences) to determine the fraction of fluorescent cells.

### RT-PCR

Total RNA was purified from the PLNs and colon of C57BL/6 wild-type and GlcNAc6ST-2$^{GFP/GFP}$ mice (13,21), and used for RT-PCR. The primers used were: 5′-TCCATACTAACGCCAGGAACG-3′ and 5′-TGGTGACTAAGGCTGGAACC-3′ for mouse GlcNAc6ST-2, 5′-TGGAATCCTGTGGCATCCATGAAAC-3′ and 5′-TAAAACGCAGCTCAGTAACAGTCCG-3′ for mouse β-actin. The PCR cycle (94°C, 30 s; 62°C, 30 s; 72°C, 1 min) was repeated 35 and 30 times for GlcNAc6ST-2 and β-actin, respectively.

### Amoxicillin (AMPC) treatment

Mice were given drinking water with or without 1 mg/ml AMPC (Sigma-Aldrich) for 10 days. The colons were mounted in OCT compound (Sakura Finetechnical) for histological analyses. A small piece of feces from each mouse was diluted 1/2000 with Luria-Bertani (LB) medium. After allowing the debris to settle, 100 μl of the supernatant was plated on a LB plate and cultured overnight at 37°C under anaerobic conditions using the Anaero-Pack System (Mitsubishi Gas Chemical). The colonies were counted to determine the antimicrobial effects of the AMPC treatment.

### Statistical analysis

Student's *t* test was used for statistical analysis.

## Results

### Generation of GlcNAc6ST-2-Cre-transgenic mice

A PCR fragment containing the Cre recombinase cDNA flanked by 50-bp homologous sequences was inserted into a 220-kb BAC carrying the gene encoding mouse GlcNAc6ST-2 by phage λ red recombinase-mediated recombineering (18,19) (Fig. 1*A*). Homologous recombination was confirmed by PCR using primer pairs designed to bind outside as well as inside the gene encoding Cre recombinase (Fig. 1*B*). Transgenic mice were generated with the

recombinant BAC and one of the founder lines, GlcNAc6ST-2-Cre, was selected for further study. The GlcNAc6ST-2-Cre-transgenic mice, maintained as hemizygotes, were healthy, fertile, and without obvious abnormalities. In addition, their PLNs were of normal size. To verify the Cre recombinase expression pattern, GlcNAc6ST-2-Cre-transgenic mice were crossed with the R26R strain (20), which expresses *lacZ* following recombination in Cre recombinase-expressing cells. Whole-mount X-gal staining of the PLNs showed that Cre recombinase was specifically expressed in the HEV-like branched structures in the GlcNAc6ST-2-Cre$^+$/R26R mice (Fig. 1*C*). Furthermore, X-gal staining of PLN tissue sections showed Cre recombinase in HEV-like blood vessels, which were easily distinguished from other blood vessels by their plump morphology (Fig. 1*D*). Lymphocyte homing to the PLNs and MLNs in GlcNAc6ST-2-Cre-transgenic mice was normal compared with that in wild-type mice (Fig. 1*E*), indicating that neither the expression of other genes encoded by the recombinant BAC nor the integration of the recombinant DNA into the mouse genome affected lymphocyte homing.

## Expression of Cre recombinase in MECA-79-reactive HEVs in GlcNAc6ST-2-Cre-transgenic mice

To examine the expression of Cre recombinase in the HEVs of GlcNAc6ST-2-Cre-transgenic mice in relation to the expression of vascular addressins, tissue sections of the secondary lymphoid organs from GlcNAc6ST-2-Cre$^+$/R26R mice were stained with mAbs MECA-79 or MECA-367 along with X-gal (Fig. 2). The MECA-79 and X-gal staining clearly colocalized in the HEVs of the PLNs, MLNs, and nasal-associated lymphoid tissues (NALTs). In contrast, the MECA-367-positive HEVs in the PP did not show X-gal staining, indicating that Cre recombinase was not expressed in the MECA-367-reactive HEVs. Interestingly, the X-gal and MECA-367 signals were clearly segregated in individual HEVs in the MLNs, further indicating that the expression of Cre recombinase and MECA-367 Ag were mutually exclusive. Since GlcNAc6ST-2 is expressed in MECA-79-reactive PLN HEVs but not in MECA-367-reactive PP HEVs (13), these results indicate that the tissue localization of Cre recombinase in the GlcNAc6ST-2-Cre-transgenic mice reflects the intrinsic expression of GlcNAc6ST-2.

## Developmental switch in Cre recombinase expression in GlcNAc6ST-2-Cre-transgenic mice

We next examined whether the expression of Cre recombinase in GlcNAc6ST-2-Cre-transgenic mice was developmentally regulated. PLNs from GlcNAc6ST-2-Cre$^+$/R26R mice were collected at various times after birth, and PLN tissue sections were doubly stained with mAbs against addressins and X-gal (Fig. 3). As reported previously (7), the expression of PNAd, which is recognized by mAb MECA-79, gradually increased after birth, and the expression of MAdCAM-1, recognized by mAb MECA-367, gradually decreased. As the MECA-79 staining became obvious ~7 days after birth, so did the expression of Cre recombinase. Only weak Cre recombinase expression was detected 4 days after birth. Thus, when crossed with flox (flanked by *loxP* sites) mice, Cre-mediated recombination occurred in the MECA-79-reactive HEVs of GlcNAc6ST-2-Cre-transgenic mice from the early neonatal stage at approximately day 7 to adulthood.

## Expression of Cre recombinase in colonic villi in GlcNAc6ST-2-Cre-transgenic mice

It has been reported that GlcNAc6ST-2 expression is restricted to HEVs (15,16). However, it was possible that other, as yet uncharacterized tissues, might also express this sulfotransferase. Thus, to determine the tissue localization of Cre recombinase in GlcNAc6ST-2-Cre-transgenic mice in detail, various tissues were collected from GlcNAc6ST-2-Cre$^+$/R26R mice and subjected to X-gal staining (Fig. 4). No staining was observed in the thymus, spleen, liver, salivary gland, heart, kidney, or pancreas. A small number of cells showed X-gal staining in the brain, lung, testis, stomach, and small intestine. In the small intestine, a few times more

cells in the jejunum than in the ileum showed X-gal staining. Fig. 4 shows X-gal staining in the ileum. At embryonic day 11.5, the GlcNAc6ST-2-Cre$^{+}$/R26R mice did not show any obvious X-gal staining, although a very minor subset of cells in the fetal heart and liver were faintly stained (H. Kawashima, unpublished observation). All of the blood vessels in the adult and fetal tissues that were examined, other than MECA79-reactive HEVs, were negative for X-gal staining. Most surprisingly, most of the colonic villi showed strong X-gal staining. No X-gal staining was observed in any tissues in the GlcNAc6ST-2-Cre$^{-}$/R26R control mice. Thus, the expression of Cre recombinase in the GlcNAc6ST-2-Cre-transgenic mice was wider than expected, with Cre recombinase being most abundantly expressed in the MECA79-reactive HEVs and colonic villi.

### Intrinsic expression of GlcNAc6ST-2 in HEVs and colonic villi

To examine whether GlcNAc6ST-2 is intrinsically expressed in the colon, tissue sections of PLNs and colon from EGFP knock-in mice (GlcNAc6ST-2$^{GFP/GFP}$ mice) were examined under confocal microscopy (Fig. 5*A*). In the knock-in mice, EGFP cDNA is inserted in-frame into the mouse GlcNAc6ST-2-coding sequence in the genome, and thus the EGFP expression reflects the intrinsic GlcNAc6ST-2 expression (13,21). We observed clear EGFP expression in the HEVs and colonic villi of the GlcNAc6ST-2$^{GFP/GFP}$ mice. No green fluorescence was seen in wild-type mice, confirming the specificity of the EGFP expression. Furthermore, RT-PCR results indicated that GlcNAc6ST-2 mRNA was expressed in both the lymph nodes and colon of wild-type mice (Fig. 5*B*). No expression of the GlcNAc6ST-2 mRNA was observed in the GlcNAc6ST-2$^{GFP/GFP}$ mice, indicating that the bands detected by RT-PCR were specific. Taken together, these results indicate that GlcNAc6ST-2 is intrinsically expressed in the colonic villi in mice and that the expression of Cre recombinase in the GlcNAc6ST-2-Cre-transgenic mice recapitulates the restricted tissue localization of GlcNAc6ST-2.

### Regulation of the colonic expression of GlcNAc6ST-2 by commensal bacteria

Since the colon contains many more bacteria than the small intestine, we next examined whether the commensal bacteria might regulate the expression of GlcNAc6ST-2 in the colon. To this end, we first treated GlcNAc6ST-2-Cre$^{+}$/R26R mice with an antibiotic agent, AMPC. After confirming that the commensal bacteria were eliminated by the AMPC treatment (Fig. 6*A*), we next performed X-gal staining of the colon. The X-gal staining was significantly reduced by the AMPC treatment, suggesting that the expression of GlcNAc6ST-2 was regulated by the commensal bacteria in the colon (Fig. 6*B*). Similarly, EGFP expression in the colonic villi of GlcNAc6ST-2$^{GFP/GFP}$ mice was significantly reduced by the AMPC treatment, confirming this notion (Fig. 6*C*).

### Characterization of cells expressing Cre recombinase in various tissues

To characterize the cells expressing Cre recombinase in tissues other than HEVs, we next performed immunohistochemical staining of the tissues in GlcNAc6ST-2-Cre$^{+}$/R26R mice using various cell type-specific Abs along with X-gal. We first used Nissl's staining to identify neurons in the brain. A small subset of Nissl's stain-positive cells in the CA3 region of the hippocampus and in the cerebral cortex were stained with X-gal, indicating that a subset of neurons expressed Cre recombinase in the brain (Fig. 7*A*, *a* and *b*). Neither the astrocyte-specific GFAP (23) nor the microgliaspecific CD11b (23) overlapped with the X-gal staining (Fig. 7*A*, *c* and *d*), further confirming this notion. No staining was observed using the isotype-matched control Abs in any of the tissues shown in Fig. 7. In the lung, the cell types expressing Cre recombinase could not be identified since they were too rare, but they were localized to the epithelium of the terminal bronchiole (Fig. 7*Be*) and alveoli (Fig. 4). In the testis, two different cell types expressed Cre recombinase, one in the seminiferous tubules and the other in the stroma. The X-gal staining in the seminiferous tubules appeared as dark dots with

extended areas of lighter color (Fig. 7*Cf*); the shapes of these cells suggested that they were Sertoli cells. The cells in the stroma appeared to be Leydig cells because of their interstitial localization between the seminiferous tubules. A subset of cells expressing GATA-4, which is expressed in Sertoli and Leydig cells in the testes (24), was positive for X-gal staining, further indicating that a subset of Sertoli cells and Leydig cells expressed Cre recombinase (Fig. 7*Cg*). Furthermore, a subset of cells expressing Sox9, another marker for Sertoli cells (25), was positive for X-gal staining (Fig. 7*Ch*), whereas cells expressing Plzf and DDX4, markers for the spermatogonia and primordial germ cells, respectively (26, 27), were not (Fig. 7*C*, *i* and *j*). In the stomach, a subset of cells expressing GATA-4 in the glandular epithelium was positive for X-gal staining (Fig. 7*Dk*). Since GATA-4 is expressed in the epithelial cells in the glandular gastric epithelium (28), this result indicates that a subset of gastric epithelial cells expressed Cre recombinase. In the jejunum, ileum, and colon, cells expressing Muc2, a marker for goblet cells (29), were positive for X-gal staining (Fig. 7*E*, *l-n*), indicating that goblet cells expressed Cre recombinase in the small intestine and colon. Staining with an anti-Muc2 Ab alone showed that goblet cells were the major population in the colonic villi (Fig. 7*Eo*), consistent with the result that most of the colonic villi showed strong X-gal staining.

## Discussion

In this study, we created a recombinant BAC-transgenic mouse line expressing Cre recombinase under control of the regulatory elements of the HEV-expressed sulfotransferase GlcNAc6ST-2. To determine the tissue distribution of Cre recombinase in this transgenic mouse line, we crossed these mice with a reporter strain, R26R (20), that expresses *lacZ* after Cre-mediated recombination. As predicted, MECA-79-reactive HEVs but not MECA-367-reactive HEVs specifically expressed Cre recombinase. No Cre recombinase expression was observed in any other blood vessels in various organs, including the thymus, spleen, liver, heart, and kidney. By performing extensive X-gal-staining experiments, we also found that Cre recombinase was expressed in the colonic villi and some other tissues in the transgenic mice.

During the early neonatal period, a developmental switch in the HEVs from the MECA-367-reactive immature phenotype to the MECA-79-reactive mature phenotype takes place (7). In relation to this developmental switch of vascular addressin expression, $CD4^+CD3^-$ inducer cells initially migrate to PLNs through an $\alpha_4\beta_7$ integrin-MAdCAM-1 interaction, whereas mature L-selectin$^+$ lymphocytes start to migrate after the induction of PNAd in PLNs (30). Thus, the developmental switch has functional consequences in determining which cell populations are attracted to the HEVs. Our results indicated that Cre recombinase started to be expressed ~7 days after birth in good correlation with the expression of PNAd recognized by the mAb MECA-79. These results indicate that the developmental switch in vascular addressin expression is at least partly due to the induction of GlcNAc6ST-2 involved in PNAd biosynthesis, since the expression of Cre recombinase recapitulated that of GlcNAc6ST-2.

The finding that the colonic expression of GlcNAc6ST-2 was regulated by the commensal bacteria suggests that signals transmitted from bacterial components or their metabolites in the colon might be partly common to those transmitted to HEVs in the developing lymph nodes. In this regard, it is of note that certain bacterial components are recognized by TLRs (31) or NOD-like receptors (32) that transmit signals leading to NF-κB activation similar to those transmitted by lymphotoxin-β receptors that are critical for lymph node neogenesis (33). Comparative studies focusing on the extracellular as well as intracellular signaling molecules in developing lymph nodes and colonic villi will help elucidate the molecular events leading to the induction of GlcNAc6ST-2.

Lymphocytes migrate to the parenchyma of lymph nodes through a multistep process in which the lymphocytes and HEVs engage in sequential adhesive interactions (3). In the first step, an essential role is played by an interaction between the homing receptor L-selectin expressed on the lymphocytes and sulfated glycans modified with the 6-sulfo sialyl Lewis X structure expressed on the HEVs, as revealed by observations of glycosyltransferaseand sulfotransferase-deficient mice, including fucosyltransferase IV and fucosyltransferase VII double-deficient mice (34), GlcNAc6ST-1 and GlcNAc6ST-2 double-deficient mice (13,14), and Core 1-β3GlcNAcT and Core2GlcNAcT double-deficient mice (11). Animals homozygous for the mutation of these enzymes develop normally and lack overt physical or reproductive defects and thus have been extremely valuable to the functional analysis of lymphocyte homing. In the second step of lymphocyte migration, chemokine presentation by heparan sulfates on HEVs has been believed to play an important role (35). However, this has not been experimentally verified in vivo, although the role of heparan sulfates in chemokine presentation on lung endothelial cells has been described (36). Our preliminary results indicate that mutant mice lacking endothelial heparan sulfates, generated by the crossing Tek-Cre-transgenic mice (37) with EXT1-flox mice (38), die as embryos (H. Kawashima, unpublished observation) and therefore are not suitable for assessing the role of heparan sulfates in lymphocyte homing. The use of the GlcNAc6ST-2-Cre-transgenic mice will facilitate the analysis of HEV-expressed genes whose pan-endothelial or ubiquitous deletion causes embryonic lethality. Our finding that the GlcNAc6ST-2-Cre-transgenic mice did not show any abnormality in our lymphocyte homing assay further supports this idea.

In contrast to previous reports that GlcNAc6ST-2 expression is specific to HEVs (15,16), we found that it was also expressed in the colonic villi and confirmed this observation by confocal microscopy of GlcNAc6ST-2$^{GFP/GFP}$ knock-in mice and RT-PCR analysis of wild-type mice. In support of our observations, it was recently reported that HEC-6ST (GlcNAc6ST-2) regulatory sequences drive *lacZ* expression in the intestinal villi in transgenic mice (17), although the authors did not confirm that the expression was authentic. In contrast, GlcNAc6ST-2 is reportedly not expressed in the normal human colon (39), which is probably due to species-specific differences in the transcriptional regulation of its gene. However, it was also reported that human colon adenocarcinoma specimens and two adenocarcinoma cell lines express GlcNAc6ST-2 (39,40), indicating that colonic epithelial cells of human origin can express GlcNAc6ST-2 under certain conditions. Our immunofluorescence studies indicated that mouse colonic villi failed to react with MECA-79 (H. Kawashima, unpublished observation), suggesting that GlcNAc-6-*O*-sulfation occurs on glycans other than extended core 1 *O*-glycans. At this point, the functional significance of the expression of GlcNAc6ST-2 in the colonic villi in mice is unclear, since no obvious abnormality was found in the histology of the colon of the GlcNAc6ST-2-deficient mice under normal conditions (H. Kawashima, unpublished observation). However, it is of note that mice lacking core 3 *O*-glycans show increased susceptibility to colitis (41) and that GlcNAc6ST-2 can act on a synthetic core 3 oligosaccharide (39,40), suggesting a possible role for GlcNAc6ST-2 in the sulfation of colonic mucins that might have anti-inflammatory roles. Further studies using animal models of colitis are needed to test this hypothesis.

Histological examinations of transgenic Cre recombinase expression, which recapitulated GlcNAc6ST-2 expression, further indicated that the expression of GlcNAc6ST-2 is broader than previously appreciated, but it is confined to specific cell types. Our results indicated that GlcNAc6ST-2 is expressed in a small subset of neurons in the CA3 region of the hippocampus and in the cerebral cortex in the brain. In the testes, two cell types, Sertoli and Leydig cells, appeared to express GlcNAc6ST-2, and cell type-specific Abs for these cells overlapped with the staining with X-gal in the GlcNAc6ST-2-Cre$^{+}$/R26R mice. In the gastrointestinal tract, GlcNAc6ST-2 expression was detected in a subset of gastric epithelial cells and in the goblet cells in the small intestine and colon. Since goblet cells are specialized for the secretion of

intestinal mucin (42), these results suggest an interesting correlation between the production of mucins and the expression of GlcNAc6ST-2 in HEV and goblet cells. Although we were unable to determine the cell types expressing GlcNAc6ST-2 in the lung, it was reported that GlcNAc6ST-2 is expressed in the airway epithelium of asthmatic lungs in sheep and that MECA-79 staining is observed in goblet cell granules in the bronchi (43). Thus, our study and this previous report suggest that goblet cells can express GlcNAc6ST-2, at least under certain conditions, although different species, organs, and pathophysiological situations were examined.

HEVs are induced ectopically at sites of chronic inflammation (9,10). For example, HEV-like vessels that react with the mAb MECA-79 are induced in the pancreas and salivary glands of NOD mice (44,45), the hyperplastic thymus of AKR mice (46), in joints with rheumatoid arthritis-induced inflammation (47), and in sites of *Helicobacter pylori*-induced inflammation (48). The GlcNAc6ST-2-Cre-transgenic mice described here, which allow conditional gene targeting in MECA-79-reactive HEVs, will be useful for assessing the gene functions in HEVs in secondary lymphoid organs as well as in these HEV-like blood vessels induced under pathophysiological situations. In addition, the expression of Cre recombinase in the colonic villi and some other tissues of the GlcNAc6ST-2-Cre-transgenic mice indicates a wider application of these mice than initially expected. Crossing them with various flox mice will be useful in studies of tissue-specific gene functions under physiological as well as pathophysiological situations, which may aid in the development of new targeted therapies.

## Acknowledgments

We thank Dr. Masayuki Oginuma (National Institute of Genetics) for providing the pBKS-CRE-FRTX2-Kan-PS and technical support and Dr. Barry L. Wanner (Purdue University, West Lafayette, IN) for providing the pKD46. We also thank Dr. Yasuyuki Imai (University of Shizuoka) for discussion, Hitomi Suzuki (National Institute of Genetics) for technical support, and Kazumi Miyawaki (University of Shizuoka) for animal care.

This work was supported in part by Grants-in-Aid for Scientific Research, Category (B) and Grants-in-Aid for Scientific Research on Priority Areas, Dynamics of Extracellular Environments from the Ministry of Education, Culture, Sports, Science and Technology, Japan (Grants 18390029 and 18060034, respectively, to H.K.), the 25th Anniversary Research Grant from the Research Foundation for Pharmaceutical Sciences, Japan (to H.K.), National Institute of Genetics Cooperative Research Program 2006-B9 (to H.K.), and National Institutes of Health Grant P01 CA71932 (to M.F.).

## References

1. Butcher EC, Picker LJ. Lymphocyte homing and homeostasis. Science 1996;272:60–66. [PubMed: 8600538]
2. von Andrian UH, Mempel TR. Homing and cellular traffic in lymph nodes. Nat. Rev. Immunol 2003;3:867–878. [PubMed: 14668803]
3. Springer TA. Traffic signals for lymphocyte recirculation and leukocyte emigration: the multistep paradigm. Cell 1994;76:301–314. [PubMed: 7507411]
4. Girard JP, Springer TA. High endothelial venules (HEVs): specialized endothelium for lymphocyte migration. Immunol. Today 1995;16:449–457. [PubMed: 7546210]
5. Streeter PR, Rouse BT, Butcher EC. Immunohistologic and functional characterization of a vascular addressin involved in lymphocyte homing into peripheral lymph nodes. J. Cell Biol 1988;107:1853–1862. [PubMed: 2460470]
6. Nakache M, Berg EL, Streeter PR, Butcher EC. The mucosal vascular addressin is a tissue-specific endothelial cell adhesion molecule for circulating lymphocytes. Nature 1989;337:179–181. [PubMed: 2911352]
7. Mebius RE, Streeter PR, Michie S, Butcher EC, Weissman IL. A developmental switch in lymphocyte homing receptor and endothelial vascular addressin expression regulates lymphocyte homing and permits $CD4^+CD3^-$ cells to colonize lymph nodes. Proc. Natl. Acad. Sci. USA 1996;93:11019–11024. [PubMed: 8855301]

8. Liao S, Ruddle NH. Synchrony of high endothelial venules and lymphatic vessels revealed by immunization. J. Immunol 2006;177:3369–3379. [PubMed: 16920978]
9. Rosen SD. Ligands for L-selectin: homing, inflammation, and beyond. Annu. Rev. Immunol 2004;22:129–156. [PubMed: 15032576]
10. Ley K, Kansas GS. Selectins in T-cell recruitment to non-lymphoid tissues and sites of inflammation. Nat. Rev. Immunol 2004;4:325–335. [PubMed: 15122198]
11. Mitoma J, Bao X, Petryanik B, Schaerli P, Gauguet JM, Yu SY, Kawashima H, Saito H, Ohtsubo K, Marth JD, et al. Critical functions of *N*-glycans in L-selectin-mediated lymphocyte homing and recruitment. Nat. Immunol 2007;8:409–418. [PubMed: 17334369]
12. Yeh JC, Hiraoka N, Petryniak B, Nakayama J, Ellies LG, Rabuka D, Hindsgaul O, Marth JD, Lowe JB, Fukuda M. Novel sulfated lymphocyte homing receptors and their control by a core1 extension β1,3-*N*-acetylglucosaminyltransferase. Cell 2001;105:957–969. [PubMed: 11439191]
13. Kawashima H, Petryniak B, Hiraoka N, Mitoma J, Huckaby V, Nakayama J, Uchimura K, Kadomatsu K, Muramatsu T, Lowe JB, Fukuda M. *N*-acetylglucosamine-6-*O*-sulfotransferases 1 and 2 cooperatively control lymphocyte homing through L-selectin ligand biosynthesis in high endothelial venules. Nat. Immunol 2005;6:1096–1104. [PubMed: 16227985]
14. Uchimura K, Gauguet JM, Singer MS, Tsay D, Kannagi R, Muramatsu T, von Andrian UH, Rosen SD. A major class of L-selectin ligands is eliminated in mice deficient in two sulfotransferases expressed in high endothelial venules. Nat. Immunol 2005;6:1105–1113. [PubMed: 16227986]
15. Hiraoka N, Petryniak B, Nakayama J, Tsuboi S, Suzuki M, Yeh JC, Izawa D, Tanaka T, Miyasaka M, Lowe JB, Fukuda M. A novel, high endothelial venule-specific sulfotransferase expresses 6-sulfo sialyl Lewis$^{x}$, an L-selectin ligand displayed by CD34. Immunity 1999;11:79–89. [PubMed: 10435581]
16. Bistrup A, Bhakta S, Lee JK, Belov YY, Gunn MD, Zuo FR, Huang CC, Kannagi R, Rosen SD, Hemmerich S. Sulfotransferases of two specificities function in the reconstitution of high endothelial cell ligands for L-selectin. J. Cell Biol 1999;145:899–910. [PubMed: 10330415]
17. Liao S, Bentley K, Lebrun M, Lesslauer W, Ruddle FH, Ruddle NH. Transgenic *LacZ* under control of *Hec-6st* regulatory sequences recapitulates endogenous gene expression on high endothelial venules. Proc. Natl. Acad. Sci. USA 2007;104:4577–4582. [PubMed: 17360566]
18. Datsenko KA, Wanner BL. One-step inactivation of chromosomal genes in *Escherichia coli* K-12 using PCR products. Proc. Natl. Acad. Sci. USA 2000;97:6640–6645. [PubMed: 10829079]
19. Copeland NG, Jenkins NA, Court DL. Recombineering: a powerful new tool for mouse functional genomics. Nat. Rev. Genet 2001;2:769–779. [PubMed: 11584293]
20. Soriano P. Generalized *lacZ* expression with the ROSA26 Cre reporter strain. Nat. Genet 1999;21:70–71. [PubMed: 9916792]
21. Hiraoka N, Kawashima H, Petryniak B, Nakayama J, Mitoma J, Marth JD, Lowe JB, Fukuda M. Core 2 branching β1,6-*N*-acetylglucosaminyltransferase and high endothelial venule-restricted sulfotransferase collaboratively control lymphocyte homing. J. Biol. Chem 2004;279:3058–3067. [PubMed: 14593101]
22. Oginuma M, Hirata T, Saga Y. Identification of presomitic mesoderm (PSM)-specific Mesp1 enhancer and generation of a PSM-specific Mesp1/Mesp2-null mouse using BAC-based rescue technology. Mech. Dev 2008;125:432–440. [PubMed: 18328678]
23. San Jose I, Garcia-Atares N, Pelaez B, Cabo R, Esteban I, Vega JA, Represa J. Reduction of glial fibrillary acidic protein-immunoreactive astrocytes in some brain areas of old hairless rhino-j mice (*hr*-rh-j). Neurosci. Lett 2001;309:81–84. [PubMed: 11502350]
24. Ketola I, Rahman N, Toppari J, Bielinska M, Porter-Tinge SB, Tapanainen JS, Huhtaniemi IT, Wilson DB, Heikinheimo M. Expression and regulation of transcription factors GATA-4 and GATA-6 in developing mouse testis. Endocrinology 1999;140:1470–1480. [PubMed: 10067876]
25. Morais da Silva S, Hacker A, Harley V, Goodfellow P, Swain A, Lovell-Badge R. Sox9 expression during gonadal development implies a conserved role for the gene in testis differentiation in mammals and birds. Nat. Genet 1996;14:62–68. [PubMed: 8782821]
26. Costoya JA, Hobbs RM, Barna M, Cattoretti G, Manova K, Sukhwani M, Orwig KE, Wolgemuth DJ, Pandolfi PP. Essential role of Plzf in maintenance of spermatogonial stem cells. Nat. Genet 2004;36:653–659. [PubMed: 15156143]

27. Fujiwara Y, Komiya T, Kawabata H, Sato M, Fujimoto H, Furusawa M, Noce T. Isolation of a DEAD-family protein gene that encodes a murine homolog of *Drosophila vasa* and its specific expression in germ cell lineage. Proc. Natl. Acad. Sci. USA 1994;91:12258–12262. [PubMed: 7991615]
28. Jacobsen CM, Narita N, Bielinska M, Syder AJ, Gordon JI, Wilson DB. Genetic mosaic analysis reveals that GATA-4 is required for proper differentiation of mouse gastric epithelium. Dev. Biol 2002;241:34–46. [PubMed: 11784093]
29. van Klinken BJ, Einerhand AW, Duits LA, Makkink MK, Tytgat KM, Renes IB, Verburg M, Buller HA, Dekker J. Gastrointestinal expression and partial cDNA cloning of murine Muc2. Am. J. Physiol 1999;276:G115–G124. [PubMed: 9886986]
30. Mebius RE, Rennert P, Weissman IL. Developing lymph nodes collect $CD4^+CD3^-LT\beta^+$ cells that can differentiate to APC, NK cells, and follicular cells but not T or B cells. Immunity 1997;7:493–504. [PubMed: 9354470]
31. Akira S, Takeda K. Toll-like receptor signalling. Nat. Rev. Immunol 2004;4:499–511. [PubMed: 15229469]
32. Shaw MH, Reimer T, Kim YG, Nunez G. NOD-like receptors (NLRs): bona fide intracellular microbial sensors. Curr. Opin. Immunol 2008;20:377–382. [PubMed: 18585455]
33. De Togni P, Goellner J, Ruddle NH, Streeter PR, Fick A, Mariathasan S, Smith SC, Carlson R, Shornick LP, Strauss-Schoenberger J, et al. Abnormal development of peripheral lymphoid organs in mice deficient in lymphotoxin. Science 1994;264:703–707. [PubMed: 8171322]
34. Homeister JW, Thall AD, Petryniak B, Maly P, Rogers CE, Smith PL, Kelly RJ, Gersten KM, Askari SW, Cheng G, et al. The α(1,3)fucosyltransferases FucT-IV and FucT-VII exert collaborative control over selectin-dependent leukocyte recruitment and lymphocyte homing. Immunity 2001;15:115–126. [PubMed: 11485743]
35. Tanaka Y, Adams DH, Hubscher S, Hirano H, Siebenlist U, Shaw S. T-cell adhesion induced by proteoglycan-immobilized cytokine MIP-1β. Nature 1993;361:79–82. [PubMed: 7678446]
36. Wang L, Fuster M, Sriramarao P, Esko JD. Endothelial heparan sulfate deficiency impairs L-selectin- and chemokine-mediated neutrophil trafficking during inflammatory responses. Nat. Immunol 2005;6:902–910. [PubMed: 16056228]
37. Koni PA, Joshi SK, Temann UA, Olson D, Burkly L, Flavell RA. Conditional vascular cell adhesion molecule 1 deletion in mice: impaired lymphocyte migration to bone marrow. J. Exp. Med 2001;193:741–754. [PubMed: 11257140]
38. Inatani M, Irie F, Plump AS, Tessier-Lavigne M, Yamaguchi Y. Mammalian brain morphogenesis and midline axon guidance require heparan sulfate. Science 2003;302:1044–1046. [PubMed: 14605369]
39. Seko A, Nagata K, Yonezawa S, Yamashita K. Ectopic expression of a GlcNAc 6-*O*-sulfotransferase, GlcNAc6ST-2, in colonic mucinous adenocarcinoma. Glycobiology 2002;12:379–388. [PubMed: 12107080]
40. Uchimura K, El-Fasakhany FM, Hori M, Hemmerich S, Blink SE, Kansas GS, Kanamori A, Kumamoto K, Kannagi R, Muramatsu T. Specificities of *N*-acetylglucosamine-6-*O*-sulfotransferases in relation to L-selectin ligand synthesis and tumor-associated enzyme expression. J. Biol. Chem 2002;277:3979–3984. [PubMed: 11726653]
41. An G, Wei B, Xia B, McDaniel JM, Ju T, Cummings RD, Braun J, Xia L. Increased susceptibility to colitis and colorectal tumors in mice lacking core 3-derived *O*-glycans. J. Exp. Med 2007;204:1417–1429. [PubMed: 17517967]
42. Specian RD, Oliver MG. Functional biology of intestinal goblet cells. Am. J. Physiol 1991;260:C183–C193. [PubMed: 1996606]
43. Rosen SD, Tsay D, Singer MS, Hemmerich S, Abraham WM. Therapeutic targeting of endothelial ligands for L-selectin (PNAd) in a sheep model of asthma. Am. J. Pathol 2005;166:935–944. [PubMed: 15743804]
44. Hanninen A, Taylor C, Streeter PR, Stark LS, Sarte JM, Shizuru JA, Simell O, Michie SA. Vascular addressins are induced on islet vessels during insulitis in nonobese diabetic mice and are involved in lymphoid cell binding to islet endothelium. J. Clin. Invest 1993;92:2509–2515. [PubMed: 7693764]

45. Faveeuw C, Gagnerault MC, Lepault F. Expression of homing and adhesion molecules in infiltrated islets of Langerhans and salivary glands of nonobese diabetic mice. J. Immunol 1994;152:5969–5978. [PubMed: 8207221]

46. Michie SA, Streeter PR, Butcher EC, Rouse RV. L-selectin and $\alpha_4\beta_7$ integrin homing receptor pathways mediate peripheral lymphocyte traffic to AKR mouse hyperplastic thymus. Am. J. Pathol 1995;147:412–421. [PubMed: 7543735]

47. Michie SA, Streeter PR, Bolt PA, Butcher EC, Picker LJ. The human peripheral lymph node vascular addressin: an inducible endothelial antigen involved in lymphocyte homing. Am. J. Pathol 1993;143:1688–1698. [PubMed: 8256856]

48. Kobayashi M, Mitoma J, Nakamura N, Katsuyama T, Nakayama J, Fukuda M. Induction of peripheral lymph node addressin in human gastric mucosa infected by *Helicobacter pylori*. Proc. Natl. Acad. Sci. USA 2004;101:17807–17812. [PubMed: 15591109]

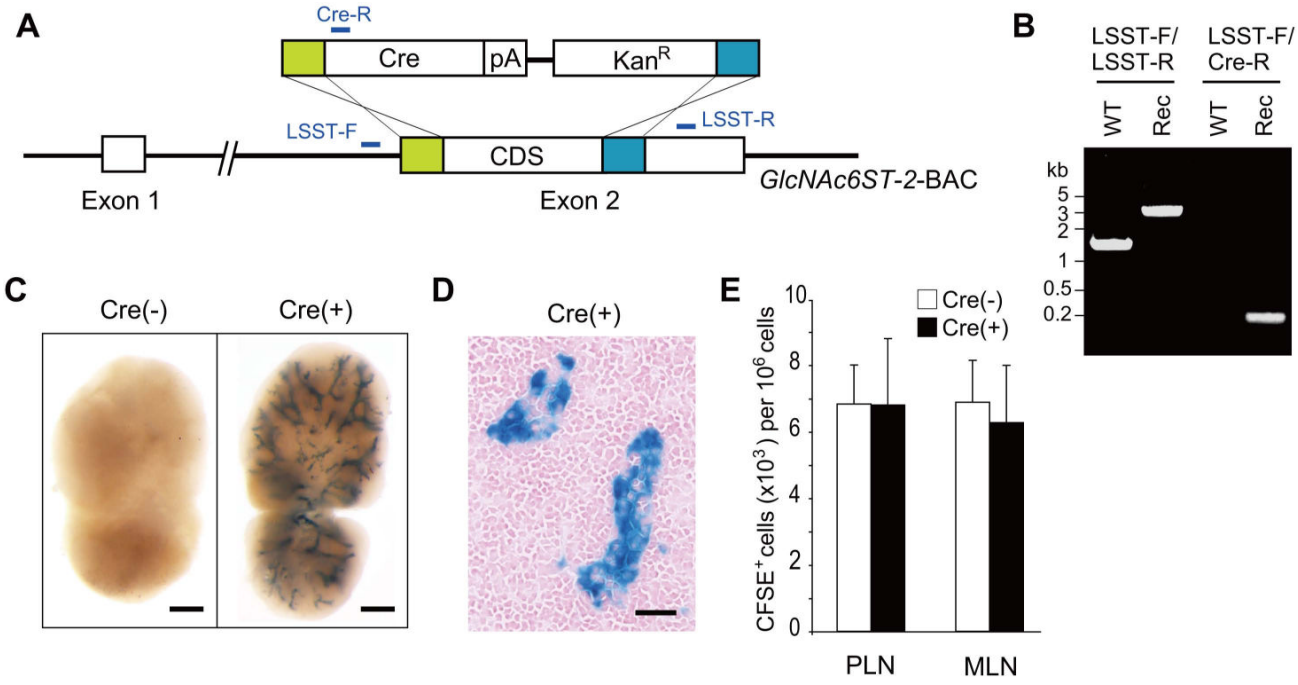


**FIGURE 1.**

Generation of GlcNAc6ST-2-Cre-transgenic mice. *A*, Construction of the recombinant BAC. Into a BAC clone harboring an ~220-kb mouse genomic DNA fragment containing the *GlcNAc6ST-2* gene was introduced a PCR fragment containing genes encoding Cre recombinase (Cre) and poly(A) (pA) and the kanamycin-resistance gene ($Kan^R$) flanked by 50-bp DNA fragments (shown by green and light blue boxes) homologous to the *GlcNAc6ST-2* gene. CDS, Coding sequence for GlcNAc6ST-2. *B*, PCR screening for the recombinant BAC. The wild-type (WT) and recombinant (Rec) BACs were subjected to PCR with primer pairs LSST-F/LSST-R and LSST-F/Cre-R shown in *A*. *C*, Whole-mount X-gal staining of PLNs from GlcNAc6ST-2-$Cre^-$/R26R ($Cre^-$) and GlcNAc6ST-2-$Cre^+$/R26R ($Cre^+$) mice. Bars, 400 μm. *D*, X-gal staining of a PLN tissue section from the GlcNAc6ST-2-$Cre^+$/R26R mouse. Bar, 30 μm. *E*, Lymphocyte-homing assay. CFSE-labeled lymphocytes were injected into the tail veins of GlcNAc6ST-2-$Cre^-$ ($Cre^-$)or GlcNAc6ST-2-$Cre^+$ ($Cre^+$) mice. One hour later, the fluorescent lymphocytes in lymphocyte suspensions from the PLNs and MLNs were quantified by flow cytometry. $n = 3$.

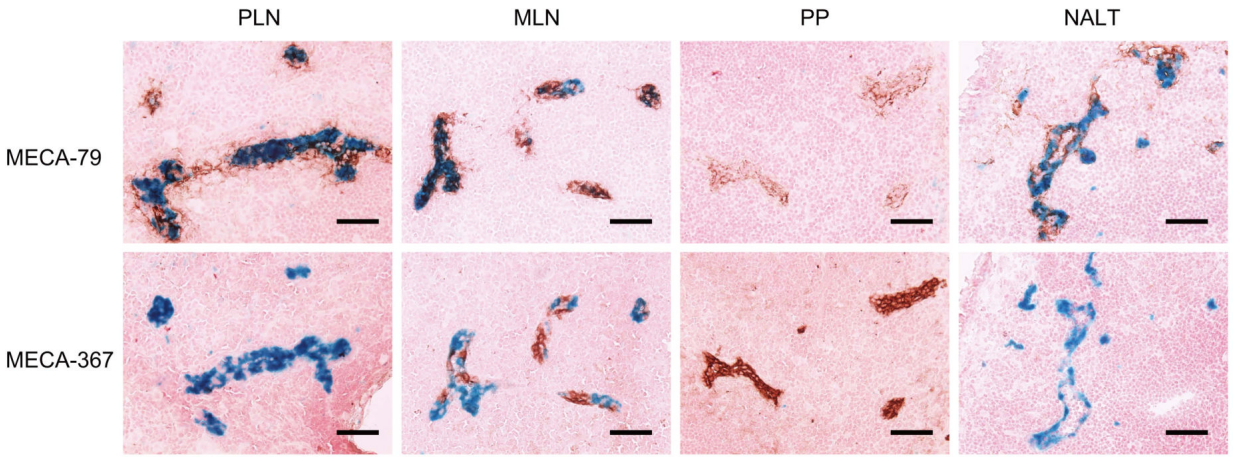


**FIGURE 2.**

Cre expression in MECA-79-reactive HEVs. Frozen sections of PLNs, MLNs, PP, and NALTs from GlcNAc6ST-2-Cre$^{+}$/R26R mice were stained with MECA-79 and MECA-367 (brown) along with X-gal (blue). Bars, 50 μm.

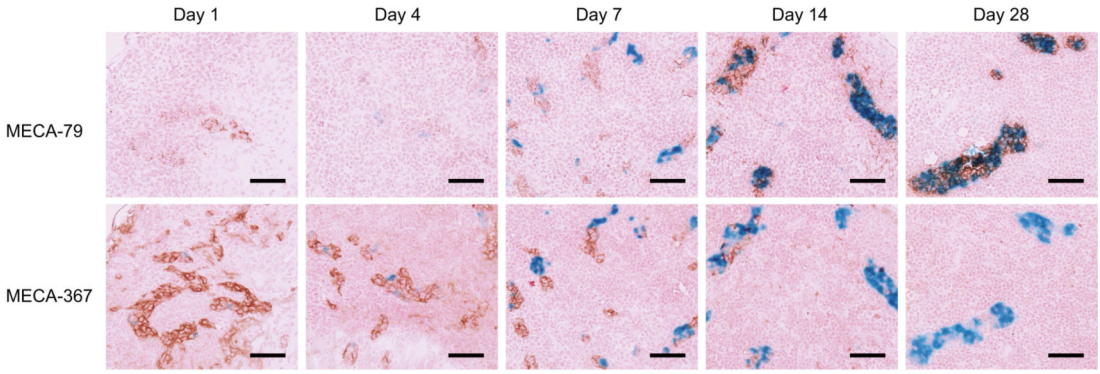


**FIGURE 3.**

Cre expression during postnatal development of HEVs. Frozen sections of PLNs from mice at various postnatal ages (days 1, 4, 7, 14, and 28) from GlcNAc6ST-2-Cre$^{+}$/R26R mice were stained with MECA-79 and MECA-367 (brown) along with X-gal (blue). Note that the X-gal staining is correlated with the developmental switch in vascular addressin expression. At least two animals were examined at each time point. Data are representative of at least three sections. Bars, 50 μm.

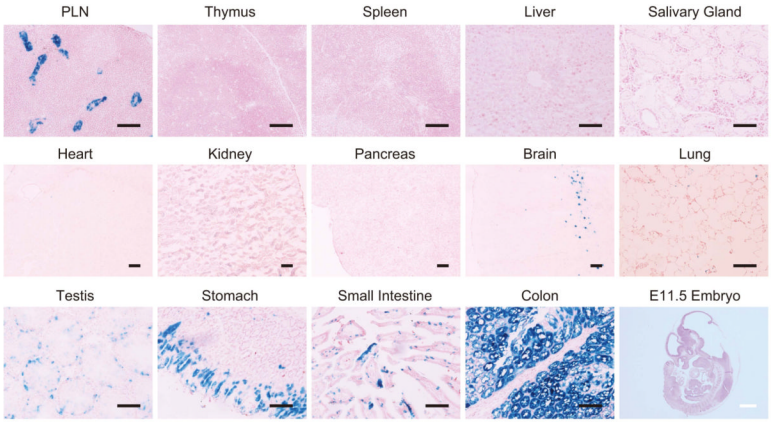


**FIGURE 4.**

Cre expression in various tissues. Frozen sections of various tissues from GlcNAc6ST-2-Cre$^{+}$/R26R mice were stained with X-gal (blue). E11.5, Embryonic day 11.5. Black bars, 100 μm; white bar, 1 mm.

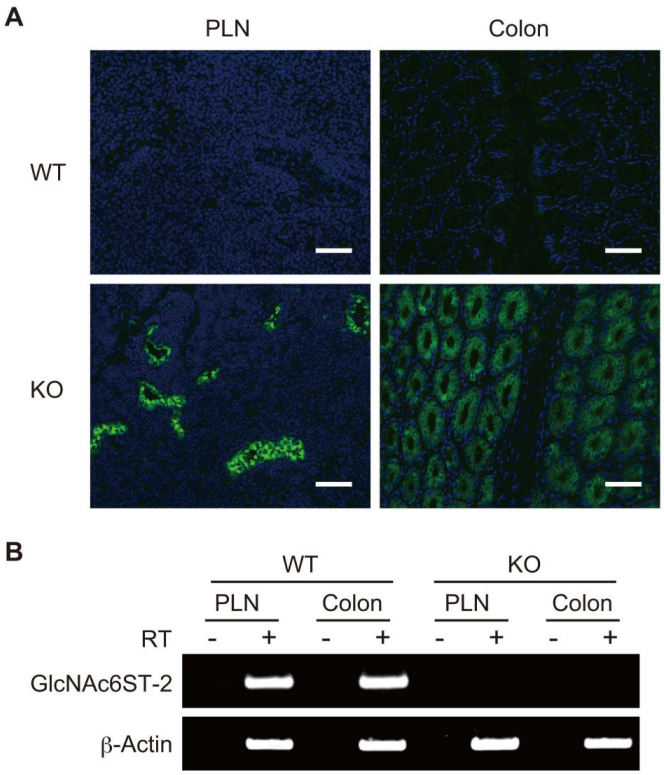


**FIGURE 5.**

Expression of GlcNAc6ST-2 in HEVs and colonic villi. *A*, Frozen sections from wild-type (WT) and GlcNAc6ST-2$^{GFP/GFP}$ (KO) mice were stained with 4′,6-diamidino-2-phenylindole and analyzed under confocal microscopy (Zeiss LSM510 META). Green fluorescence is from GlcNAc6ST-2-EGFP chimeric protein (13,21). Bars, 50 μm. *B*, Single-stranded cDNA prepared in the presence (+) or absence (-) of reverse transcriptase (RT) from the PLNs or colon of wild-type or GlcNAc6ST-2$^{GFP/GFP}$ (KO) mice was used as a template for PCR to detect the expression of GlcNAc6ST-2 and β-actin.

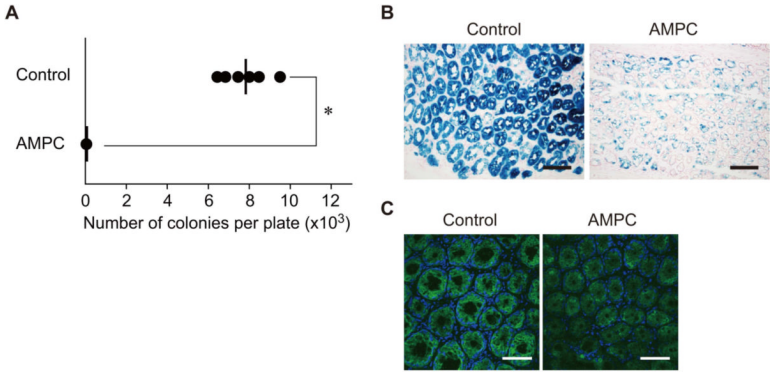


**FIGURE 6.**

Regulation of the colonic expression of GlcNAc6ST-2 by commensal bacteria. *A*, Number of commensal bacteria in the colon of GlcNAc6ST-2-Cre$^+$/R26R mice treated with (AMPC) or without (Control) AMPC. The number of colonies appearing on LB plates under anaerobic conditions was counted as described in *Materials and Methods*. The vertical bar represents the mean of the six determinations. *, $p < 0.01$. *B*, Effects of AMPC on the expression of *lacZ* in the colon of GlcNAc6ST-2-Cre$^+$/R26R mice. Data are representative of three independent experiments. Bars, 100 μm. *C*, Effects of AMPC on the expression of EGFP in the colon of GlcNAc6ST-2$^{GFP/GFP}$ mice. Data are representative of three independent experiments. Bars, 50 μm.

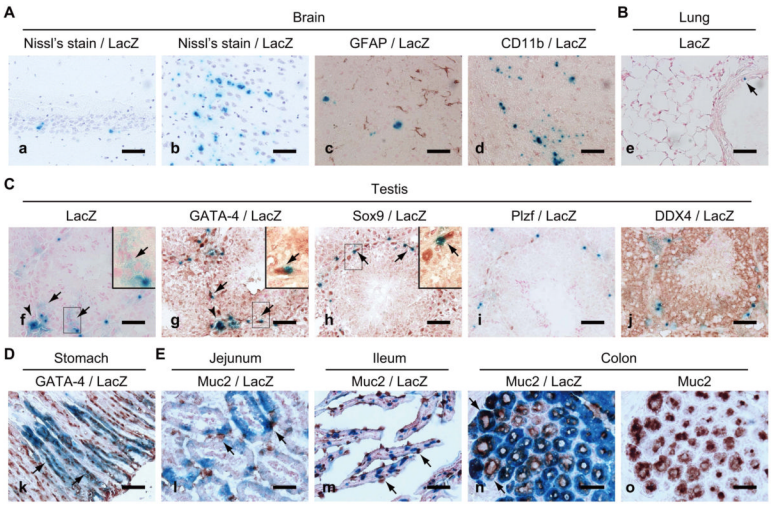


**FIGURE 7.**

Characterization of cells expressing Cre recombinase in various tissues. Frozen sections of various tissues from GlcNAc6ST-2-Cre$^{+}$/R26R mice were stained as follows: *A*, Brain was stained with 0.1% cresyl violet (*a* and *b*; purple), anti-GFAP pAb (*c*; brown), or anti-CD11b mAb (*d*; brown) along with X-gal (blue). *a*, CA3 region of the hippocampus; *b-d*, cerebral cortex. *B*, Lung was stained with X-gal (*e*). Arrow indicates an X-gal-reactive cell in the epithelium of the terminal bronchiole. *C*, Testis was stained with X-gal alone (*f*) or with anti-GATA-4 (*g*), anti-Sox9 (*h*), anti-Plzf (*i*), or anti-DDX4 (*j*) pAbs. Arrows in *f* indicate cells with extended areas of light X-gal staining. Arrows in *g* and *h* indicate cells reactive with both anti-GATA-4 pAb and X-gal and anti-Sox9 pAb and X-gal, respectively. Arrowheads in *f* and *g* indicate cells in the stroma. *D*, Stomach was stained with anti-GATA-4 pAb along with X-gal (*k*). Arrows indicate cells reactive with both anti-GATA-4 pAb and X-gal. *E*, Jejunum, ileum, and colon were stained with anti-Muc2 pAb along with X-gal (*l-n*). In *o*, colon was stained with anti-Muc2 pAb alone. Arrows indicate cells reactive with both anti-Muc2 pAb and X-gal. Bars: *panels*,50 μm; *inset*s, 20 μm.